# A Calculation Method For Mineral Reserves Based On Multi-point Geostatistics

Yongzhi Wang[1,2*], Mengrou Yu[2], Hui Wang[3], and Baojuan Wang[1]

[1] *School of Geography Science and Geomatics Engineering, Suzhou University of Science and Technology, Suzhou, China*
[2] *School of Civil and Surveying & Mapping Engineering, Jiangxi University of Science and Technology, Ganzhou, China*
[3] *Provincial Geomatics Center of Jiangsu, Nanjing, China*
[*] *Corresponding author. E-mail: gisstarww@qq.com*

*Received: Jun. 10, 2022; Accepted: Sept. 15, 2022*

To improve the accuracy of the calculation for the current mineral resource reserves, a calculation method for mineral resource reserves based on multi-point geostatistics was proposed. The new method, including four major steps, focuses on calculating resource reserves of ore body accurately for rational development and utilization of mineral resources. To represent the spatial geometric relationship of the ore body accurately, a three-dimensional irregular tetrahedron voxel (3D ITV) model construction method for the ore body is proposed first. Second, a tetrahedron voxel grade model built by the mineral reservation calculation oriented multi-point geostatistics method is proposed. The construction of 3D training image, definition of data template with N-order adjacency voxels, construction of search trees and conditional probability extraction of data event are conducted in this step. Finally, the resource reserves of the ore body are calculated on the basis of the tetrahedron voxel grade model. A calculation experiment of copper reserves is conducted to demonstrate the validity of the new method. The new method can be meaningful to the exploration, development, and utilization of mineral resources.

**Keywords:** Mineral reserve calculation, multi-point geostatistics, 3D irregular tetrahedron voxel model, 3D training images


http://dx.doi.org/10.6180/jase.202312_26(12).0013

## 1. Introduction

With the development of smart mining and sustainability, the efficiency of mineral resource development and utilization must be improved [1, 2]. Accurate calculation of available reserves of geological objects is necessary for the comprehensive development and utilization of mineral resources [3, 4]. However, the accuracy of the available reserves calculated by existing methods is reduced significantly when the geological objects are complicated [5, 6]. Therefore, exploring the calculation method for complex geological objects is greatly important [7, 8].

At present, the calculation methods of mineral reserves contain two categories, namely, geologic block methods and geostatistics methods [9–12]. In the geologic block method, the ore body is manually divided into uneven parts (named blocks) according to the ore geological condition, and then the thickness, volume and reserves of each block are calculated by the weighted or arithmetic mean method to obtain the resource reserves of the whole ore body [13]. For the geologic block method, only several sample grades are selected as the average grade and the overall spatial variability of the grade is ignored, causing deviations in the calculation of mineral reserves and reducing the accuracy of calculation results [14, 15].

The geostatistics methods consider mineralization phenomena as random variables that related to spatial location on the basis of probability statistics, and the variogram is used to represent the correlation and variability of the spatial regionalized variables [16–18]. The characteristics of the spatial regionalized variables are considered in the geostatistics methods, and the data of the exploration work can be used extensively [19–22]. However, the variogram can only calculate the correlation between two points in space. Thus, the geostatistics methods have difficulty characterizing the spatial structure of complex geological bodies and reproducing the geometric form of complex ore bodies [23]. Furthermore, the accuracy of experimental variogram is low, if the sampling data is sparse or unevenly distributed in the early stages of mining area. Thus, the correctness and accuracy of the correlation between two spatial points are reduced, resulting in the low accuracy of results [24, 25].

In a word, the overall spatial variability of grade of ore body is not considered in the geologic block methods reducing the accuracy of calculation results. For geostatistics methods, the lack of exploration work results in great uncertainty in the calculation of the variogram. Multi-point geostatistics uses voxels as the basic unit to represent the 3D geometry of the ore body, and adopts a sequential non-iterative algorithm. In addition, the variation characteristics of the spatial regionalized variables are represented by training images instead of the variogram. Thus, multi-point geostatistics can improve the accuracy of assessment results [26, 27].

On the basis of the single normal equation simulation (Snesim) algorithm of the multi-point geostatistics [28], the calculation method for mineral reserves based on multi-point geostatistics is proposed. The basic idea and details of the new method are delivered in Section 2. In Section 3, a case study of the calculation of a copper mine is conducted by using the new method. In Section 4, we deliver our conclusions on the effect and accuracy of the new method. Our results show that the new method can improve the calculation accuracy of mineral reserves.

## 2. Methodology

### 2.1. Basic Idea and Overall Design

The current calculation methods of mineral reserves can only represent the spatial correlation of two points losing the 3D geometric relationship information of a complex ore body, reducing the calculation accuracy of mineral reserves. the multi-point geostatistics can simulate unknown points to describe the continuity and variability of spatial regionalized variables, which is useful to simulate the grade information of the mineral resources. The grade information of regular hexahedron voxels can be fused into three-dimensional irregular tetrahedron voxel (3D ITV) model to construct the 3D training images. Compared with the existing models, the 3D ITV model can reflect the internal spatial structure and details of the complex ore body, and provide voxel model support for a high-precision reserve calculation. Furthermore, the 3D training images can represent the relationships between spatial structure characteristics of ore body and are mined to obtain the conditional probability distribution of the grade in the unknown area by using the improved Snesim algorithm. Thus, 3 the multi-point geostatistics can improve the accuracy of mineral reserve calculation.

The overall design of the new method involves three major steps (Fig. 1). First, a 3D ITV model is constructed on the basis of the multi-source geological data. An unevaluated tetrahedron voxel (UTV) model is built by filling real boreholes into the 3D ITV model. Second, a tetrahedron voxel grade model built by the mineral reservation calculation oriented multi-point geostatistics method is proposed. The construction of 3D training image, definition of data template with N-order adjacency voxels, construction of search trees and conditional probability extraction of data event are conducted in this step. Finally, the resource reserves of the ore body are calculated on the basis of the tetrahedron voxel grade model.

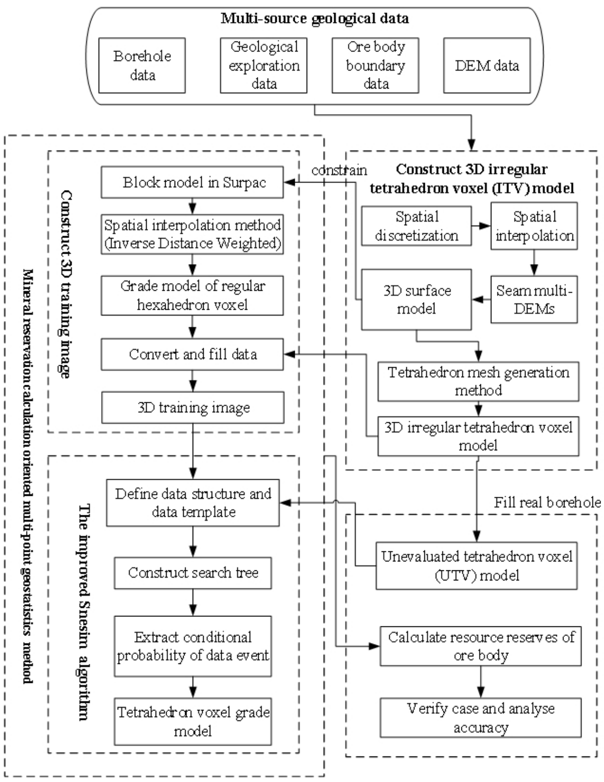


**Fig. 1.** Flowchart of the overall design.

### 2.2. Construction of 3D ITV Model

As a spatial geometric relationship carrier of internal attributes, such as the grade of ore bodies, the 3D ITV model can realize the integration of the internal attributes and spatial geometry. This integration is a key step in the calculation of mineral reserves. A construction method of the 3D ITV model for mineral reserve calculation is proposed, which includes spatial geometric modeling and grade assignment of voxels. The 3D ITV model provides voxel model support for a high-precision reserve calculation.

The main process of 3D ITV model construction involves three steps. First, multi-source data, such as borehole data, digital elevation model (DEM) data, and ore body boundary data, are integrated. Second, the seaming multi-DEMs and boundary representation (B-Rep) methods are used to construct the 3D surface model. Finally, TetGen, a tetrahedron mesh generation method of 3D spatial entities, is used to divide the 3D surface model into a 3D ITV model [29]. The grade information obtained from the borehole sampling should be assigned to voxels of the 3D ITV model, which can be used as the evaluation object of the multi-point geostatistic methods. The main process of the grade assignment of voxels is as follows. On the basis of the orifice coordinate, orifice radius, orifice elevation, and the maximum depth of the borehole, the borehole is expanded into a borehole cylinder with grade information. Then, the spatial geometric relationship between the borehole cylinder and the voxels is judged. If they intersect, the grade information is assigned to the voxels of the 3D irregular tetrahedron voxel model. By performing the above process on all borehole data, the grade assignment of voxels is completed. Then, an UTV model can be built for the mineral resource reserve calculation. In the UTV model, voxels with grade values are called conditional data, while other voxels with unknown grade values are called unevaluated voxels. The grade values of unevaluated voxels are estimated by using the improved Snesim method of multi-point geostatistics.

To organizing and managing irregular voxels of the UTV model efficiently, the half-edge data structure is expanded by adding voxel classes and correlative information [30]. In the expanded half-edge data structure, each face is composed of two reverse half-faces [31]. Each half-face, called the Cell, contains four members. The voxel is called the Tetrahedron, to which the Cell belongs. The adjacent half-face of the Tetrahedron is called Next. Then, the vertex set of the Cell is called Points. The other reverse half-face is called Pair, which shares the same face with the Cell. Thus, any point, face, or voxel in the UTV model can be founded through any Cell.

### 2.3. Mineral Reservation Calculation Oriented Multi-point Geostatistics Method

Drawing lessons from the simulation calculation ideas of the classical Snesim method in multi-point geostatistics, we propose a mineral reservation calculation oriented multi-point geostatistics method, including construction of 3D training image and improvement of Snesim algorithm. The improved Snesim algorithm involves definition of data template with N-order adjacency voxels, the search tree construction and extraction of conditional probability of data event. 3D training images can quantitatively represent the spatial structure characteristics of the ore body, and provide a transcendental spatial structure support for the method. The data template with N-order adjacency voxels can extract spatial features of spatial regionalized variables. Search trees can store and classify all patterns of the data templates in 3D training images.

#### *2.3.1. Construction of 3D Training Image*

The 3D training image is not faithful to the structural information of the actual geological body, as it is only a conceptual model of the geological body [32]. The 3D training image can be used as a geological prior knowledge. A construction method of 3D training images for the reserve calculation is presented. The method includes two steps. First, on the basis of the method of constructing the 3D ITV model, the geometric model of the 3D training images is constructed. Then, grade assignment of the geometric model is performed. The process of grade assignment in 3D training images mainly includes two steps: the generation of the grade model of regular hexahedron voxel and grade evaluation of 3D ITV model. The selected grid unit of 3D training images fits the size of the UTV model. The selected grid units are 3D ITV model taking the tetrahedron as the basic unit. The grade model of regular hexahedron voxel is constructed by using the spatial interpolation methods of the Surpac software. Then, the grade values of a regular hexahedron voxel are assigned to 3D ITVs through Boolean operation among spatial objects. Afterward, 3D training images for the calculation of ore body reserves are generated.

The construction of the grade model of regular hexahedron voxel has three steps. First, the size of regular hexahedron voxels is determined by factors, such as evaluation precision and calculation efficiency. Then, the ore body is divided into hexahedron grids to establish a regular hexahedron voxel model. Finally, the appropriate spatial interpolation method, such as 3D Kriging method, is selected to assign the grade of the regular hexahedron voxel model on the basis of the grade information of the borehole sampling data.

On the basis of the grade model of regular hexahedron voxel, the core of grade assignment for a 3D ITV model is to determine whether a hexahedron and a tetrahedron intersect. Then, the grade values of hexahedrons are assigned to the 3D ITV model. Thus, 3D training images taking the tetrahedron as the basic unit are constructed. The 3D training image can well simulate the boundary characteristics and grade information of ore bodies. The process of grade assignment is described as follows.

(1) The geometric model of a tetrahedron voxel and the grade model of regular hexahedron voxel are loaded.

(2) The grade model of regular hexahedron voxel is traversed, and the spatial topological relation between each hexahedron and tetrahedron is judged. First, to accelerate the speed of judging spatial topological relation, the positional relationship of bounding boxes is judged. If they are separate from one another, the assignment operation can be ended directly, which can further reduce unnecessary operations of the calculation of spatial topological relation. The intersection of the hexahedron and the tetrahedron includes three forms, namely, the intersection of the hexahedron and the tetrahedron, the tetrahedron contained by the hexahedron, and the hexahedron contained by the tetrahedron. The grade value of the regular hexahedron voxel is assigned to the tetrahedron voxel to which the regular hexahedron voxel intersects.

(3) The arithmetic mean of grades of multiple hexahedrons is considered as the grade value of a tetrahedron when there is a spatial relationship (containing, intersecting and being contained) between the tetrahedron and multiple hexahedrons at the same time.

(4) When the hexahedron voxels are traversed, the grade assignment of all tetrahedron voxels is completed, in other words, the 3D training images representing the grade distribution can be generated.

#### *2.3.2. Improvement of Snesim Algorithm*

The basic unit of the 3D training image is tetrahedron, which cannot be mined by the Snesim algorithm. Therefore, the improved Snesim algorithm defines a data template with tetrahedron as basic unit, namely, data template with N-order adjacency voxels first. Then, the 3D training image is mined by data template with N-order adjacency voxels to construct a search tree. Finally, conditional probabilities of data events from the search tree are extracted to calculate the grade value of unevaluated voxels.

**Definition of data template with n-order adjacency voxels** The data template, which is composed of multiple adjacent data units, e.g., voxels, can extract the spatial features of spatial regionalized variables. This template is marked as $\tau_n$, and it represents the spatial geometric model composed by m vectors ($\tau_n$={$h_i$;i=1,2,. . . . . . ,m}). If the center position of $\tau_n$ is assumed to be u, then the other positions of $\tau_n$ are $u_i$=u+$h_i$. Fig. 3(a) is a 3 × 3 two-dimensional data template whose $u_i$ is determined by the center point (u) and eight vectors ($h_i$). In Fig. 2(a), the vectors are represented by grid points. Fig. 3(b) is a 3 × 3 × 3 3D data template whose central voxel (u) is represented by a black grid. The 3D voxels around the central voxel $u_i$ represent the position of the spatial vectors, which are represented by white grids in Fig. 2(b).

The data template with N-order adjacency voxels about unevaluated voxels is defined by considering the significance of the data template and the spatial structure correlation of the geological body. N-order adjacency voxels are coplanar with unevaluated voxels. The adjacency voxels, which are coplanar with N-order adjacency voxels, are sequentially searched. After coplanar searches are performed n times, the obtained set of adjacency voxels is used as a data template. To obtain N-order adjacency voxels around the Tetrahedron in the improved half-edge data structure, the first-order adjacency voxels of the Tetrahedron are searched. Information on the first-order adjacency voxels is stored in the attribute of the AdjacentTetrahedron. Then, the second-order adjacency voxels of the Tetrahedron are determined. Afterward, the N-order adjacency voxels of the Tetrahedron are searched. Some adjacency voxels are reduced correspondingly if the boundary voxel is touched. Given the boundary voxels in the adjacency voxels of Tetrahedron, the size of the data template is not fixed.

The data template with N-order adjacency voxels is suitable for the complex 3D ITV model. The credibility of the evaluation results can be improved by using the N-order adjacency voxels with a strong spatial correlation as the data template. This template extends and explores the definition of a data template. Thus, new ideas are provided to the application and development of multi-point geostatistics in various research fields.

**Construction of search trees** The data template mines the 3D training images by constructing search trees, and the construction process uses a three-layer iteration. In the first iteration, each tetrahedron voxel of the 3D training images is traversed to obtain the N-order adjacency voxels set. The adjacency voxels with grade values are stored, and the ID of voxel is stored uniquely in a data template (called templateTetraID). In the second iteration, the current tetra-

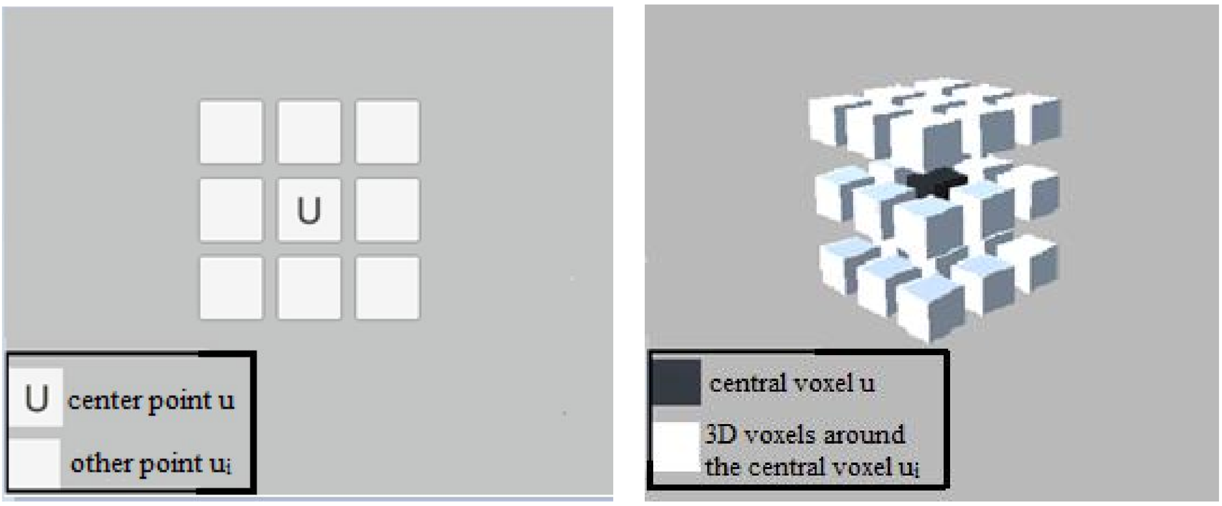


(a) (b)

**Fig. 2.** Illustration of regular data templates, (a) 3 × 3 two-dimensional data template, (b) 3 × 3 × 3 3D data template.

hedron voxel is traversed to obtain the N-order adjacency voxels on the basis of the ID. The N-order adjacency voxels are called adjacentTetrahedron. In the third iteration, the grade values of each N-order adjacency voxels are compared with the grade value stored in the corresponding node of the search tree. The node is called currentTreeNode. If the grade values are the same, the node number (named couter) is increased by 1. Otherwise, a new node called treeNode is created. The search trees are constructed after each tetrahedron of the 3D training images mined by the data template.

**Conditional probability extraction of data event** For the conditional probability extraction of data event, the tetrahedron voxel grade model is generated after the UTV model are evaluated. First, the N-order adjacency voxels are used as the data template to mine the UTV model. Consequently, search trees are constructed. Then, a data event centered on the unevaluated voxel is extracted sequentially. The conditional probability of the data event is extracted from the search tree. Finally, the grade value of the unevaluated voxel is calculated on the basis of the conditional probability. The detailed process is described as follows.

(1) A simulation path is determined firstly when the unevaluated voxel of UTV model is evaluated. The storage order of voxels in the UTV model is considered as a simulation path. The simulation path is not a random path. Along the simulation path, the voxel with grade is not evaluated, and the unevaluated voxel is evaluated.

(2) The 3D training images and the UTV model are read. The improved half-edge data structure is used to organize and manage the model.

(3) A customized data template with N-order adjacency voxels is used to mine the 3D training images. Then, the search trees are constructed.

(4) The N-order adjacency voxels of each unevaluated voxel are taken according to the simulation path. Some conditional data exist in N-order adjacency voxels. Then, the data event is composed by N-order adjacency voxels and unevaluated voxels. The conditional probability of data event is found from the search tree.

(5) In the process of obtaining a conditional probability distribution from 3D training images on the basis of data events, two issues may occur. First, the evaluation can be obtained from the conditional data when N-order adjacency voxels contain some conditional data. Second, N-order adjacency voxels do not contain conditional data. In other words, no voxel with a grade is present. The unevaluated voxel is estimated by the overall grade distribution probability in the 3D training images.

(6) After obtaining the conditional probability distribution, the grade value range corresponding to the conditional probability is considered as the value interval of a grade. In addition, the voxel numbers of grade values are counted from the value interval in the 3D training images. Then, the conditional probability of each grade value appearing in value interval is calculated. For example, when the value interval of grade is

from 1.5% to 2.1% in the 3D training images, the number of voxels is counted. Then, the number of voxels are 10, 35, 20, 60, 40, 18, 39, respectively. In addition, the conditional probabilities of the seven grade values are calculated by statistical data. The conditional probabilities are 0.045, 0.158, 0.09, 0.27, 0.18, 0.081, and 0.176, respectively.

(7) The conditional probability of each grade in the value interval is added up according to the value, and the cumulative probability of the last grade is 1. The conditional probabilities of the grade values that appear in Step 6 are added up. Then, the cumulative probabilities are 0.045, 0.203, 0.293, 0.563, 0.743, 0.824, and 1 respectively.

(8) To ensure the randomness of the evaluation results, a random number in the range of 0–1 is generated. The grade evaluation results of voxels are selected by comparing the random number with the cumulative probability. The cumulative probability described in Step 7 is taken as an example. When the random number is 0.55 that is between 0.293 and 0.563, the corresponding cumulative probability is 0.563 and the voxel grade evaluation result is 1.8%. When the random number is 0.88 that is between 0.824 and 1.0, the corresponding cumulative probability is 1.0 and the voxel grade evaluation result is 2.1%. The evaluation result is used as the conditional data for the subsequent evaluation process.

(9) The next unevaluated voxel is traversed along the simulation path, and Steps 4–8 are repeated until all unevaluated voxels are assigned grade values. Then, the tetrahedron voxel grade model is generated.

### 2.4. Reserves Calculation

On the basis of the spatial geometric relationship and grade values of the tetrahedron voxel grade model, the tetrahedron volume, the average weight of the ore and the grade value are multiplied. Then, the resource reserve of each tetrahedron is calculated. The reserves of the ore body are obtained through adding up tetrahedron reserves.

Given that the basic geometric units of the tetrahedron voxel grade model are tetrahedrons, the vertex coordinates of the tetrahedron are set to $P_1(x_1, y_1, z_1)$, $P_2(x_2, y_2, z_2)$, $P_3(x_3, y_3, z_3)$, $P_4(x_4, y_4, z_4)$. The volume of the tetrahedron voxel ($V_i$), the quantity of ore of the tetrahedron ($Q_i$), and the mineral reserves of the tetrahedron voxel ($P_i$) are calculated by Formulas 1–3, respectively. The total mineral reserves of the ore body is the sum of mineral reserves of voxels in the tetrahedron voxel grade model.

$$V_{terahedron} = \frac{1}{6}\begin{vmatrix} x_1 & y_1 & z_1 & 1 \\ x_2 & y_2 & z_2 & 1 \\ x_3 & y_3 & z_3 & 1 \\ x_4 & y_4 & z_4 & 1 \end{vmatrix} \tag{1}$$

$$Q_i = V_i \times D \tag{2}$$

$V_i$ is the volume and D is the average density.

$$P_i = Q_i \times C_i \tag{3}$$

$C_i$ is the voxel grade.

## 3. Case study

### 3.1. Study Area and Data Set

The study area is I-3 ore body that belongs to Heiniudong copper deposit in Jiulong country, Sichuan Province. The I-3 ore body is taken as the research object (Fig. 3). The I-3 ore body is taken from a large-scale annular ore belt, which is found in the mineralization alteration zone of metamorphic rocks in the early proterozoic Liwu rock group.

Evident fractures are not observed in the study area. The deformations during the period of metamorphism, especially the tectonic deformation of brittleness-ductileness and ductility before mineralization, are fully developed. The fault zones of the river bed and the mountain body are approximately parallel main fault zones in the mine [33]. The strike is 310°-320°, the length is 775 meters, and the dip angle is 23°-30° in the I-3 ore body. The axial direction of the reverse side of I-3 ore body is 45°-225°. Overall, the strike of I-3 ore body is slightly steeper in the shallow part, and becomes gradual toward the deep part [34]. These characteristics show that the inclination of I-3 ore body does not change uniformly. The middle part is thick, and both sides are thin in the I-3 ore body. These characteristics show that the grade of I-3 ore body does not change uniformly. The natural types of ore in the I-3 ore body mainly includes brecciated, massive and quasi-massive types. Ore minerals are mainly composed of pyrrhotite and chalcopyrite. They also contain a small amount of molybdenite and pyrite [35].

Data set contains borehole data, contour lines, copper grade of borehole, and exploration line data in study area. The boreholes are sparsely distributed, with only 26 groups of borehole data. The borehole data cannot fully represent the geological characteristics of the study area, which results in the difficulty of accurate calculation of reserves.

### 3.2. 3D ITV Model of I-3 Ore Body

The I-3 ore body is taken as the research object. The research data, such as the borehole data, contour lines, cop-

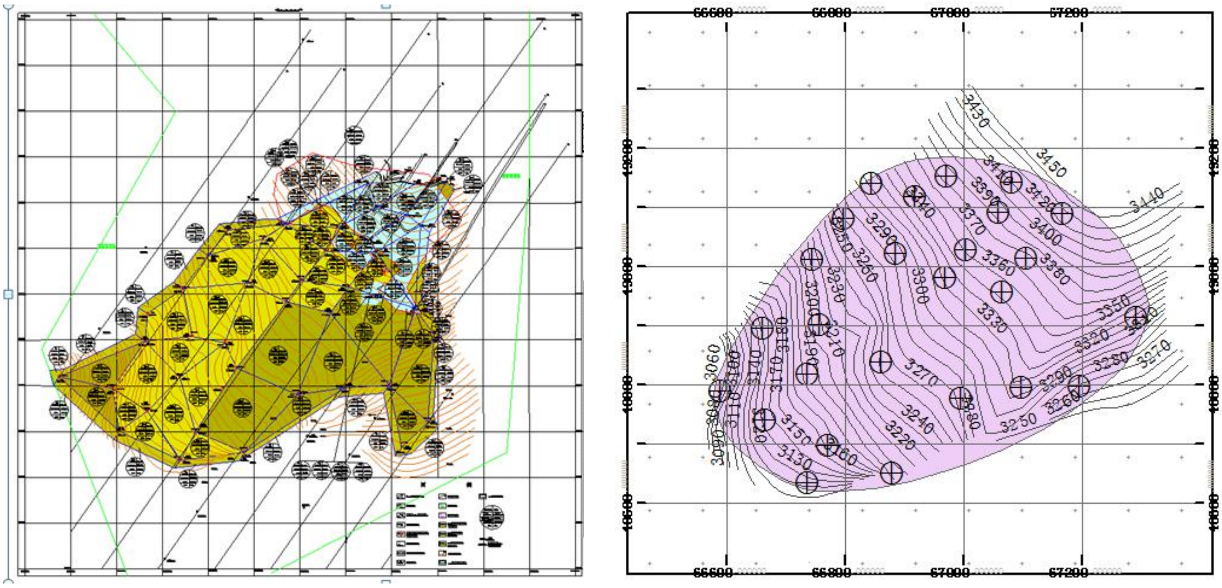

(a) (b)

**Fig. 3.** Information of I-3 ore body, (a) Horizontal projection drawing, (b) Selected research area (the figure contains the ore boundary, contour lines and borehole distribution.).

per grade of borehole, and exploration line data, are organized and processed. Given the constraints of the delineated boundary, the 3D ITV model is constructed by setting the voxel number to 6 on the basis of the DEM data and borehole data. The model contains approximately 50 thousand tetrahedron voxels (Fig. 4(a)). To illustrate the spatial structures and morphological characteristics of voxels effectively, Fig. 4(b) only shows the visualization of the local details of screening tetrahedron voxels after magnification.

### 3.3. 3D Training Image of I-3 Ore Body

X is set to 5 meters, Y is set to 2.5 meters, and Z is set to 1.25 meters when the sampling data of the I-3 ore body is analyzed. Then, a regular hexahedral voxel model with 120 thousand regular hexahedrons is obtained. Next, the inverse distance weighted (IDW) method is used to estimate the copper grade of each regular voxel of the model. Then, a grade model of regular hexahedron voxel is generated. The distribution of the copper grade is visualized (as shown in Fig. 5) by performing the volume rendering for the grade values of voxels. Finally, the grade information of 120 thousand regular hexahedrons is assigned to the 3D ITV model containing 50 thousand tetrahedrons through the intersection judgment. Through the above steps, the 3D training images are generated.

### 3.4. Copper Reserve Calculation of I-3 Ore Body

The UTV model with some conditional data is constructed by assigning the grade information of 26 groups of borehole data to the 3D ITV model. The search tree is constructed through the 5th-order adjacency voxels as the data template. Moreover, unevaluated grades are evaluated by extracting the conditional probability distribution of unevaluated voxels. Then, the tetrahedron voxel grade model of the I-3 ore body is obtained. On the basis of the tetrahedron voxel grade model, the copper grade value contained in each tetrahedron is calculated. The calculated average grade of copper is 3.156%, and the copper reserves are 228,573 tons. Comparing the results of ordinary Kriging method and the new method with the average grade of 2.88% after mining , the result error of the new method is smaller. Thus, the new method is effective in simulating grade information, and guarantee the accuracy of reserve calculation.

## 4. Conclusion

The calculation method for mineral reserves based on multipoint geostatistics is proposed in this paper. The main achievements of this research are as follows. First, the 3D ITV model is constructed to represent the 3D geometric shape. This model represents the spatial geometric relationship more effectively. Second, the construction of the 3D training image, and the definition of the data template with N-order adjacency voxels and search tree construction for the 3D ITV model are realized. Thus, the spatial correlation of multiple points is represented. Third, the grade evaluation and mineral reserves of the 3D ITV model are calculated. The accuracy of the evaluated grade by the

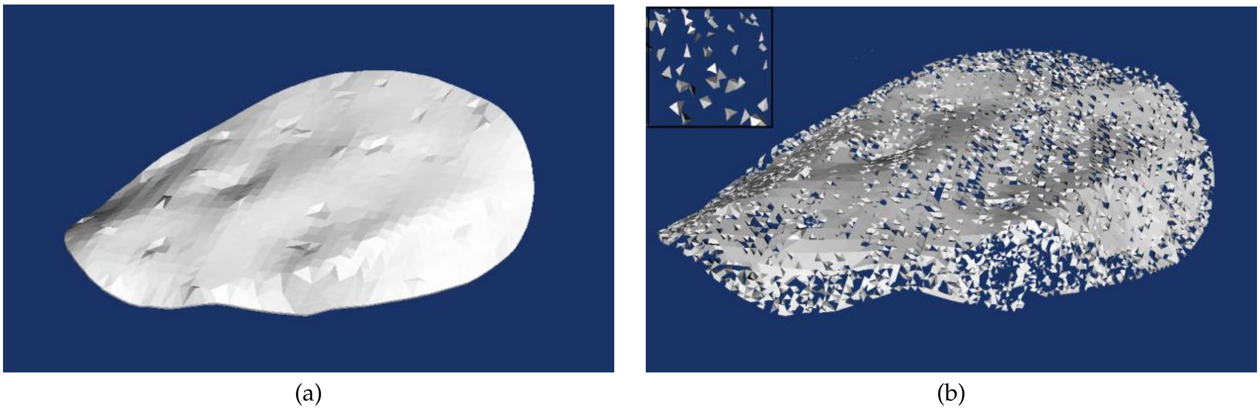


**Fig. 4.** 3D voxel model of I-3 ore body, (a) All voxel models, (b) Screening voxel models.

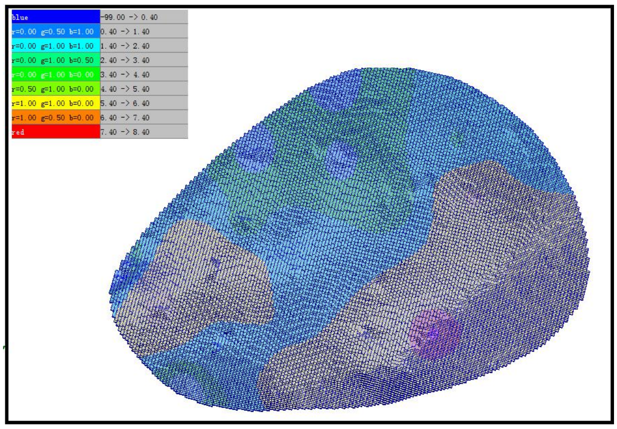


**Fig. 5.** Grade model of regular hexahedron voxel of I-3.

new method is improved. Thus, the calculation accuracy of grade distribution and mineral reserves is high. The validity of the new method is represented by taking a copper ore body to calculate copper reserves. The results show that the new method is more efficient than the existing methods in calculating the mineral reserves.

The new method can more accurately represent the spatial structure, 3D spatial geometric relationship, and spatial distribution of the grade. Therefore, the new method can realize the high-precision calculation of mineral reserves. The new method has important theoretical and reference significances in calculating other mineral resources.

## Acknowledgement

This study is supported by the National Natural Science Foundation of China (No. 42061061), the Youth Jinggang Scholars Program in Jiangxi Province (No. QNJG2020046) and the Program of Qingjiang Excellent Young Talents, Jiangxi University of Science and Technology (No. JXUSTQJBJ2018002). The authors would also like to acknowledge the contributions of Jacqueline Wah to the spelling and grammar check for this paper.

## Declaration of interests

The authors declare that they have no known competing financial interests or personal relationships that could have appeared to influence the work reported in this paper.

## References

**[1]** X. Huang, X. Li, K. Hu, Y. Liu, and D. Liu, (2012) *"Status and Achievement of the Green Mine in China"* **International Proceedings of Chemical Biological & Environmental Science and Development (ICESD)**:

**[2]** A. Valero, A. Valero, and G. M. Mudd. "Exergy-a useful indicator for the sustainability of mineral resources and mining". In: *SDIMI Conference Gold Coast*. 2009.

**[3]** F.-W. Wellmer, J. D. Becker-Platen, D. J. Shields, J. A. Briskey, K. J. Schulz, J. P. Mosesso, L. R. Horwitz, C. G. Cunningham, P. F. Langhammer, W. J. Bawiec, et al., (2007) *"Proceedings for a Workshop on Deposit Modeling, Mineral Resource Assessment, and Their Role in Sustainable Development"* **Guizhou Ethnic Studies**: DOI: 10.3133/cir1294.

**[4]** M. Khaidir Noor. "Ore Reserve Estimation of Saprolite Nickel Using Inverse Distance Method in PIT Block 3A Banggai Area Central Sulawesi". In: ***979***. 1. Cited by: 0; All Open Access, Gold Open Access. 2018. DOI: 10.1088/1742-6596/979/1/012047.

**[5]** R. d. S. Machado and J. F. C. L. Costa, (2019) *"Field parametric geostatistics-an alternative to tackle gold grade estimations"* **Revista Escola de Minas** ***72***(1): 167–172. DOI: 10.1590/0370-44672018720085.

**[6]** B. Samanta, S. Bandopadhyay, and R. Ganguli, (2002) *"Data segmentation and genetic algorithms for sparse data division in Nome placer gold grade estimation using neural network and geostatistics"* **Exploration and Mining Geology *11***(1-4): 69–76. DOI: 10.2113/11.1-4.69.

**[7]** D. Silva and J. Almeida, (2017) *"Geostatistical methodology to characterize volcanogenic massive and stockwork ore deposits"* **Minerals *7***(12): DOI: 10.3390/min7120238.

**[8]** S. Strebelle, (2002) *"Conditional simulation of complex geological structures using multiple-point statistics"* **Mathematical Geology *34***(1): 1–21. DOI: 10.1023/A:1014009426274.

**[9]** C. Castañón, D. Arias, I. Diego, A. Martin-Izard, and Y. Ruiz, (2017) *"Resource and reserve calculation in seam-shaped mineral deposits; a new approach: "The pentahedral method""* **Minerals *7***(5): DOI: 10.3390/min7050072.

**[10]** H. Anhar and F. Khalifani. *Evaluation of Mineral Reserves*. 2018.

**[11]** R. Wang, L. Li, D.-W. Zhou, Z.-G. Lu, H.-M. Deng, and S.-A. Ke, (2019) *"Calculation of Rare Earth Ore Reserves by Geostatistics"* **Chinese Rare Earths *40***(2): 35–41. DOI: 10.16533/J.CNKI.15-1099/TF.20190001.

**[12]** S. Haldar. "Chapter 8 - Mineral Resource and Ore Reserve Estimation". In: *Mineral Exploration*. Ed. by S. Haldar. Boston: Elsevier, 2013, 137–155. DOI: https://doi.org/10.1016/B978-0-12-416005-7.00008-8.

**[13]** L. Shu, Y. Cheng, L. Wang, J. Jiang, Q. Zhai, and S. Kong, (2011) *"Research on influence of geological factors on gas storage in coal seam"* **China Safety Science Journal *21***(02):

**[14]** J. Hou and G. Guo, (1993) *"Theory and Apply of Statistical Prediction of Deposits and Geostatistics"* **Metallurgical Industry Press**: 325–327.

**[15]** X. Gong, (2019) *"3D Geological Modeling and Resource Estimation of Laotianzhuang Manganese Deposit in Chongqing"* **Chengdu University of Technology**:

**[16]** L. Coppa, E. Green, and C. Quan, (1984) *"Geostatistics for Resource/Reserve Estimation."*

**[17]** F. Bastante, J. Taboada, L. Alejano, and C. Ordóñez, (2005) *"Evaluation of the resources of a slate deposit using indicator kriging"* **Engineering Geology *81***(4): 407–418. DOI: 10.1016/j.enggeo.2005.08.003.

**[18]** G. Wang, Z. Pang, J. B. Boisvert, Y. Hao, Y. Cao, and J. Qu, (2013) *"Quantitative assessment of mineral resources by combining geostatistics and fractal methods in the Tongshan porphyry Cu deposit (China)"* **Journal of Geochemical Exploration *134***: 85–98. DOI: 10.1016/j.gexplo.2013.08.004.

**[19]** *A Study of Coupling Surface Network to Reservoir Simulation Model in a Large Middle East Field*. ***All Days***. SPE North Africa Technical Conference and Exhibition. SPE-127976-MS. 2010. DOI: 10.2118/127976-MS. eprint: https://onepetro.org/SPENATC/proceedings-pdf/10NATC/All-10NATC/SPE-127976-MS/1764218/spe-127976-ms.pdf.

**[20]** S. KASMAEE, J. GHOLAMNEJAD, A. YARAHMADI, and H. MOJTAHEDZADEH, (2010) *"Reserve estimation of the high phosphorous stockpile at the Choghart iron mine of Iran using geostatistical modeling"* **Mining Science and Technology (China) *20***(6): 855–860. DOI: https://doi.org/10.1016/S1674-5264(09)60295-7.

**[21]** A. E. Tercan, B. Ünver, M. A. Hindistan, G. Ertunç, F. Atalay, S. Ünal, and Y. Killioğlu, (2013) *"Seam modeling and resource estimation in the coalfields of western Anatolia"* **International Journal of Coal Geology *112***: 94–106. DOI: 10.1016/j.coal.2012.10.006.

**[22]** K. Modis, S. Stavrou, N. Terezopoulos, and D. Vattis, (2008) *"Geostatistics versus inverse distance squares in ore reserves estimation: Comparative case study in copper ore body in Cyprus"* **Transactions of the Institutions of Mining and Metallurgy, Section A: Mining Technology *117***(1): 48–52. DOI: 10.1179/174328607X228866.

**[23]** S. Talesh Hosseini, O. Asghari, S. A. Torabi, and M. Abedi, (2020) *"An Optimum Selection of Simulated Geological Models by Multi-Point Geostatistics and Multi-Criteria Decision-Making Approaches; a Case Study in Sungun Porphyry-Cu deposit, Iran"* **Journal of Mining and Environment *11***(2): 481–503. DOI: 10.22044/JME.2020.8710.1757.

**[24]** L. Hu and T. Chugunova, (2008) *"Multiple-point geostatistics for modeling subsurface heterogeneity: A comprehensive review"* **Water Resources Research *44***(11): DOI: 10.1029/2008WR006993.

**[25]** G. Mariethoz and J. Caers. *Multiple-point Geostatistics: Stochastic Modeling with Training Images*. ***9781118662755***. Cited by: 313. 2014, 1–364. DOI: 10.1002/9781118662953.

**[26]** T. ZHANG, (2008) *"Incorporating Geological Conceptual Models and Interpretations into Reservoir Modeling Using Multiple-Point Geostatistics"* **Earth Science Frontiers** ***15***(1): 26–35. DOI: https://doi.org/10.1016/S1872-5791(08)60016-0.

**[27]** P. W. Mirowski, D. M. Tetzlaff, R. C. Davies, D. S. McCormick, N. Williams, and C. Signer, (2009) *"Stationarity scores on training images for multipoint geostatistics"* **Mathematical Geosciences** ***41***(4): 447–474. DOI: 10.1007/s11004-008-9194-0.

**[28]** S. Strebelle, (2002) *"Conditional simulation of complex geological structures using multiple-point statistics"* **Mathematical Geology** ***34***(1): 1–21. DOI: 10.1023/A:1014009426274.

**[29]** H. Si, (2015) *"TetGen, a delaunay-based quality tetrahedral mesh generator"* **ACM Transactions on Mathematical Software** ***41***(2): DOI: 10.1145/2629697.

**[30]** Y. Wang, H. Zhao, Y. Sheng, and N. Kang, (2015) *"Construction and application of 3d geological models for attribute-oriented information expression"* **Journal of Applied Science and Engineering** ***18***(4): 315–322. DOI: 10.6180/jase.2015.18.4.01.

**[31]** P. Boguslawski, C. M. Gold, and H. Ledoux, (2011) *"Modelling and analysing 3D buildings with a primal/dual data structure"* **ISPRS Journal of Photogrammetry and Remote Sensing** ***66***(2): 188–197. DOI: 10.1016/j.isprsjprs.2010.11.003.

**[32]** Y. Yin, C. Zhang, and S. Li, (2013) *"Principle, method and application of multi-point geostatistics"* **Geology press**:

**[33]** J. Li, M. Wang, F. Wang, P. Yao, J. Liang, G. Tang, X. Zhu, G. Ma, G. Zou, Z. Shen, et al., (2010) *"Characteristics of ductile shear-type disseminated ores in Heiniudong copper deposit, Jiulong County, Sichuan Province"* **Mineral Deposits** ***29***(5): 853–868. DOI: 10.1360/972010-741.

**[34]** M. Chen, J. Ding, X. Zhu, G. Ma, P. Yao, and J. Li, (2013) *"Geological and geochemical characteristics and its ore-forming mechanism of Heiniudong copper deposit, Jiulong, Sichuan"* **Mineral Resources and Geology** ***27***(6): 479–486.

**[35]** F. Cao, (2016) *"The study on Geological characteristics and Genesis of Heiniudong Cu deposit in Jiulong country, Sichuan Province, China"* **Chengdu University of Technology**: